

# Catalysis Science & Technology

Accepted Manuscript



This is an *Accepted Manuscript*, which has been through the Royal Society of Chemistry peer review process and has been accepted for publication.

*Accepted Manuscripts* are published online shortly after acceptance, before technical editing, formatting and proof reading. Using this free service, authors can make their results available to the community, in citable form, before we publish the edited article. We will replace this *Accepted Manuscript* with the edited and formatted *Advance Article* as soon as it is available.

You can find more information about *Accepted Manuscripts* in the [Information for Authors](#).

Please note that technical editing may introduce minor changes to the text and/or graphics, which may alter content. The journal's standard [Terms & Conditions](#) and the [Ethical guidelines](#) still apply. In no event shall the Royal Society of Chemistry be held responsible for any errors or omissions in this *Accepted Manuscript* or any consequences arising from the use of any information it contains.

## Tailoring the selectivity in glycerol oxidation by tuning the acid-based properties of Au catalysts

Cite this: DOI: 10.1039/x0xx00000x

Alberto Villa,<sup>a</sup> Sebastiano Campisi,<sup>a</sup> Khaled. M. H. Mohammed,<sup>b,c,g</sup> Nikolaos Dimitratos,<sup>c,e,f</sup> Floriana Vindigni,<sup>d</sup> Maella Manzoli,<sup>d</sup> Wilm Jones,<sup>e,f</sup> Michael Bowker<sup>e,f</sup> Graham Hutchings,<sup>c</sup> and Laura Prati,<sup>a,\*</sup>

Received 00th January 2012,  
Accepted 00th January 2012

DOI: 10.1039/x0xx00000x

www.rsc.org/

Supported gold nanoparticles are very effective catalysts for the selective oxidation of glycerol which represents an important bio-derived feedstock. In this paper we report that the effect of the acid/base properties, especially the acid site density, of these catalysts is the key factor available to tune the selectivity. A range of supported AuPt catalysts have been prepared by sol immobilization using acidic (H-Mordenite, SiO<sub>2</sub>, MCM-41, sulfated ZrO<sub>2</sub>) and basic (NiO, MgO) oxides as supports. In particular, using MCM-41 as support, a high selectivity to glyceraldehyde, an important labile intermediate, was found.

### Introduction

Glycerol is a highly functionalized molecule, derived from lipids transesterification in the production of biodiesel, that is recognized as a promising chemical building block for the synthesis of fine chemicals.<sup>1</sup> For instance, the selective oxidation of glycerol has been shown to produce valuable products such as glyceraldehyde (GLYALD) glyceric acid (GLYA), dihydroxyacetone (DHA) and tartronic acid (TA).<sup>2</sup> Supported noble metal nanoparticles have been used as catalysts for this reaction when molecular oxygen is employed as the oxidant even though the nature of the metal and the experimental conditions appeared of primary importance to determine the activity and to direct the selectivity to the desired products.<sup>3</sup> In particular gold nanoparticles are both active and selective for this reaction.<sup>4</sup> However, the main limitation of gold monometallic catalysts appears to be the requirement for basic conditions.<sup>4</sup> From an industrial point of view working under non-basic conditions provides a great advantage and numerous efforts have been devoted to solve this problem. Recently it was found that the catalytic oxidation of glycerol with gold catalysts can be carried out avoiding the use of a basic environment.<sup>5</sup> In particular, alloying Au with Pt is possible to obtain an effective catalytic system in terms of activity and selectivity even in the absence of a base.<sup>5a,5b,5f</sup> However, these studies clearly showed that the support greatly affected the activity and the selectivity. Indeed, using an acidic support, H-Mordenite, an enhancement in both the activity and the selectivity to C<sub>3</sub> products occurs (glyceric and tartronic acid), compared to similar AuPt particles supported on activated carbon and TiO<sub>2</sub>.<sup>5a</sup> More recently, it has been shown

that also by using basic supports such as MgO and hydrotalcite it is possible, as well, to obtain a high selectivity to C<sub>3</sub> products by a careful tuning of the reaction conditions, specifically by controlling the reaction temperature.<sup>5b,5e</sup> From these studies it can be summarised that a new-generation of bifunctional gold-based catalysts can be prepared, where the acid/base properties of the support play a crucial role, affecting both activity and selectivity of the reaction.

The aim of the present study is to clarify the effect of the acid site nature and strength (Lewis and/or Brønsted) and acid site density on the activity and selectivity of Au-Pt nanoparticles supported on acidic supports in the base-free glycerol oxidation.

### Results and discussion

Four acidic oxides with different acid/base properties, i.e. H-Mordenite, SiO<sub>2</sub>, MCM-41, sulfated ZrO<sub>2</sub> (S-ZrO<sub>2</sub>), have been used as support, and compared to two basic supports (MgO and NiO). Bimetallic AuPt catalysts were prepared by sol immobilization technique through a two steps procedure,<sup>5a</sup> which ensures the formation of alloyed bimetallic particle and controlled particle size. The catalytic tests were carried out in the base free glycerol oxidation at 80°C (0.3M glycerol, glycerol/metal=500 mol/mol, 3 atm O<sub>2</sub>, T= 80 °C). The activity and the selectivity of the catalysts are reported in table 1.

Table 1: Base free glycerol oxidation at 80°C

Catalyst	Activity mol (AuPt mol) <sup>-1</sup> h <sup>-1</sup> a	Selectivity (%) <sup>b</sup>										NH <sub>3</sub> adsorbed amount (μmol/m <sup>2</sup> ) <sup>c</sup>
		GLYA	GLYALD	TA	DHA	C3	GLYCA	OXA	FA	C2+C1		
AuPt/MgO	657	21	7	1	12	41	8	6	43	59	-	
AuPt/NiO	283	51	10	8	16	85	7	2	8	17	-	
AuPt/MCM-41	228	35	46	1	16	98	1	1	-	2	0,34	
AuPt/SiO <sub>2</sub>	156	61	16	1	18	96	2	1	-	3	0,72	
AuPt/H-Mordenite	105	53	19	-	23	95	1	2	1	4	2,68	
AuPt/S-ZrO <sub>2</sub>	113	57	19	3	17	96	1	1	1	3	2,96 <sup>b</sup>	

Reaction conditions: 0.3M glycerol, glycerol/metal=500mol/mol, 3atm O<sub>2</sub>, T=80°C a) Mol of glycerol converted per hour per mol of metal, calculated after 15 min reaction b) Selectivity calculated at 30% conversion. GLYA=glyceric acid; GLYALD=glyceraldehyde; TA=tartronic acid; DHA=dihydroxyacetone; GLYCA=glycolic acid; OXA= oxalic acid; FA= formic acid; C2= oxalic acid and glycolic acid; C1= formic acid. c) Amount of NH<sub>3</sub> adsorbed under an equilibrium pressure of 5 Torr. Amount of NH<sub>3</sub> obtained subtracting the contribution of Lewis sites

First of all, the higher activity of the basic support compared to the acidic ones is not surprising. In terms of activity, as expected, the presence of a basic support such as MgO (isoelectric point of 10.4) increased the activity.<sup>5b</sup> It is well recognized that the mechanism of glycerol oxidation consists in an oxidative dehydrogenation. The presence of a base enhances the β-hydride abstraction, which is the limiting step for this reaction.<sup>3</sup> To be noted that AuPt/MgO is able to maintain high selectivity toward glyceric acid even at high conversion only if the temperature is maintained below 25°C.<sup>5b</sup> ICP analysis performed on the reaction media, evidenced the presence of Mg in solution. Mg could be a sacrificial base, promoting both H-abstraction and the successive desorption of the Mg-glycerate, therefore limiting the deactivation phenomena due to strongly adsorbed byproducts. AuPt NPs on MgO was a very active catalyst, exhibiting an initial activity (657 converted mol of glycerol (AuPt mol)<sup>-1</sup> h<sup>-1</sup>), superior to that observed when the same AuPt NPs were immobilized on NiO (283 mol of glycerol (AuPt mol)<sup>-1</sup> h<sup>-1</sup>) and on the acidic supports (113, 105, 156, 228 (mol of glycerol (AuPt mol)<sup>-1</sup> h<sup>-1</sup>), for S-ZrO<sub>2</sub>, H-Mordenite, SiO<sub>2</sub> and MCM41, respectively) (Table 1). However, no direct correlation between acid/base properties and catalytic activity was found.

Interestingly, AuPt NPs on MCM41 showed limited deactivation phenomena, if compared to AuPt supported on S-ZrO<sub>2</sub>, SiO<sub>2</sub> and H-Mordenite showing a reaction profile similar to AuPt/NiO and AuPt/MgO (S1), determining a sort of

breakout line between acid and basic supports. Moreover, recycling experiments carried out just by filtering the catalyst and adding fresh solution of glycerol confirmed the good stability of AuPt/MCM41 at least after six runs in terms of activity but also selectivity (S2). The mesostructure of MCM-41 was maintained after recycling tests, as confirmed by SAXRD analyses (S3).

From a selectivity point of view, AuPt NPs on acidic supports appeared the best choice. Indeed, as shown in Table 1, using acidic supports a higher selectivity to C3 compounds (GLYA + GLYALD + TA + DHA) (~95%) has been obtained whereas basic supports, in particular MgO, promoted C-C bond cleavage to C2 and C1 products in high amount (59%).

In addition, the formation of glyceraldehyde in significant yield was observed with the usage of acidic supports as a labile compound. Particularly AuPt/MCM-41 showed the highest selectivity to glyceraldehyde (46% at 30% conversion). To the best of our knowledge this is the first time that glyceraldehyde has been detected in such a great amount. The presence of glyceraldehyde was also confirmed by <sup>13</sup>C-NMR analysis of the reaction mixtures (S4).

It can be noted that the higher selectivity to glyceraldehyde showed by MCM-41 is related to a lower production of glyceric acid compared to the other acidic supports.

By decreasing the reaction temperature from 80°C to 60°C and to 40°C the activity of the catalyst decreased, as expected with an initial activity of 228, 173 and 112 (mol of glycerol (AuPt mol)<sup>-1</sup> h<sup>-1</sup>), respectively (S5). However by decreasing the

reaction temperature, the selectivity to glyceraldehyde increased, giving the best result at 40°C (55% at 30% conversion) (S5).

Focusing on AuPt NPs supported on acidic supports and in order to understand the influence of the nature of the support on the catalytic activity and selectivity, a detailed characterization of the morphology and of the surface properties of the catalysts was performed.

TEM data collected on the samples revealed a good AuPt dispersion in all the catalysts (Fig.1). EDS analysis showed that AuPt nanoparticles are alloyed particles (S6). Moreover, the size of AuPt particles is not significantly affected by the support, with a mean diameter of 6.2-7.5 nm (S7). Therefore we can conclude that the impact of particle size is negligible on the catalytic performance of AuPt based catalysts tested in this work.

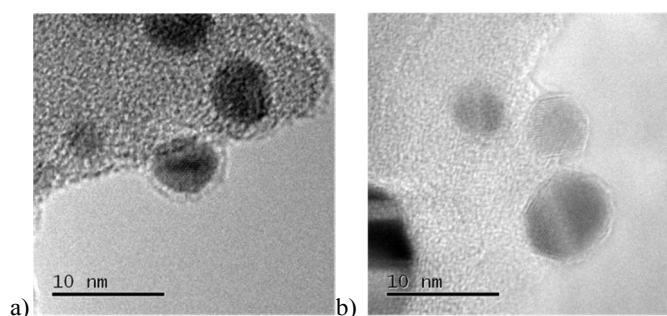
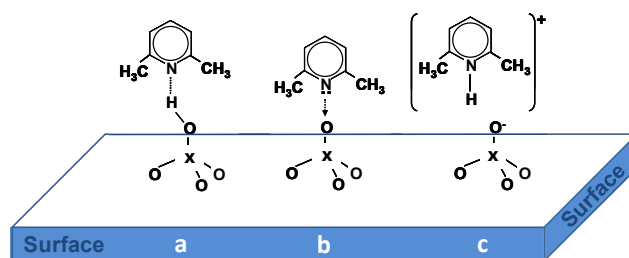


Fig. 1. Representative TEM images of a) AuPt/MCM-41 b) AuPt/SiO<sub>2</sub>

Therefore, we focused on the investigation of the acidic properties of AuPt nanoparticles supported on SiO<sub>2</sub>, MCM-41, S-ZrO<sub>2</sub> and H-Mordenite by means of FTIR spectroscopy. 2,6-Dimethylpyridine (2,6-DMP) has been used as probe molecule. The adsorption/desorption of such probe is suitable because (i) it allows us to identify both Lewis and Brønsted acidic centers present at the surface and above all (ii) it can distinguish Lewis and/or Brønsted sites of different acidic strength.<sup>6</sup> Moreover, when the base is probing Brønsted sites, it is adsorbed in its 2,6-dimethylpyridinium form (2,6-DMPH<sup>+</sup>). This species yields two strong and well recognizable 8a-8b bands (ring stretching modes) centered at 1640-1655 cm<sup>-1</sup> and at about 1630 cm<sup>-1</sup>, respectively. Whereas, Lewis bound and H-bonded species give typically three bands in the 1620-1580 cm<sup>-1</sup> range.<sup>7</sup> In particular, the  $\nu_{8a}$  mode, that in the liquid phase appears at 1594 cm<sup>-1</sup>, is very sensitive and allows us the identification of different types of 2,6-DMP adsorption on solids. In fact, when the  $\nu_{8a}$  wavenumber is higher than 1625 cm<sup>-1</sup>, it characterizes protonated species (2,6-DMPH<sup>+</sup>) whereas lower wavenumber correspond to coordinated or H-bonded species (DMPL). The 2,6-DMP molecule interacting by H-bond (a) and adsorbed on Lewis (b) and Brønsted (c) sites is represented in Scheme 1.

Therefore, to describe the adsorption/desorption of 2,6-DMP, we focus on the bands in the 1650-1550 cm<sup>-1</sup> spectral range. The FTIR spectra, normalized with respect to the surface area and collected after the interaction with 2 mbar of 2,6-DMP at

room temperature (r.t.) and during the outgassing, are shown in Figure 2.



Scheme 1. 2,6-DMP molecule interacting by H-bond (a) and adsorbed on Lewis (b) and Brønsted (c) sites exposed at the surface of the catalysts.

Upon adsorption of 2 mbar of 2,6-DMP at r.t. (red curves), complex bands in the 1605-1580 cm<sup>-1</sup> range due to the  $\nu_{8a}$  and  $\nu_{8b}$  of liquid like and H-bonded 2,6-DMP are formed on all catalysts. As expected, no Lewis and Brønsted acidity was observed for AuPt/MCM-41 and AuPt/SiO<sub>2</sub>. Beside the liquid like form, the 2,6-DMP probe interacts with these systems exclusively through H-bonding with surface silanol groups. Moreover, the  $\nu_{8a}$  mode is highly blue shifted at 1605 cm<sup>-1</sup> (that is a position typically observed when the probe interacts with Lewis sites) confirming the acid character of silanols. The observed bands gradually decrease in intensity after 30' outgassing at increasing time at the same temperature (blue curves). The higher stability of the bands related to AuPt/MCM-41, if compared with those detected on AuPt/SiO<sub>2</sub>, is due to the presence of mesopores, in fact the H-bonded 2,6-DMP is gradually removed by prolonging the outgassing time (data not shown for the sake of brevity).

On the other hand, the catalyst supported on sulphated zirconia showed both Lewis (1602 cm<sup>-1</sup>) and Brønsted acid sites (1628 and 1648 cm<sup>-1</sup>) whereas for AuPt/H-Mordenite we observed almost exclusively Brønsted acidity (bands at 1633 and 1647 cm<sup>-1</sup>). The apparent absence of Lewis sites for H-Mordenite is ascribed to residual water adsorbed on the surface due to the mild pre-treatment of the samples (drying at 80°C). It should be noted that glycerol oxidation was carried out in water that implies the Lewis sites to be masked.

The adsorption/desorption of 2,6-DMP allowed us to identify the different acidic centers present at the surface of the catalysts, however there is no clear correlation between the nature of the sites and the trend observed as for the catalytic activity and selectivity. Recently, Stosic et al. reported on the influence of the acid-base properties of zirconia and titania based materials on the dehydration reaction of glycerol.<sup>8</sup> In particular, authors demonstrated that the catalytic activity was dependent not only from the nature of the acid sites, but also from the total acidity of the catalysts. Based on these premises, we carried out quantitative studies of the acid sites present on the different samples.

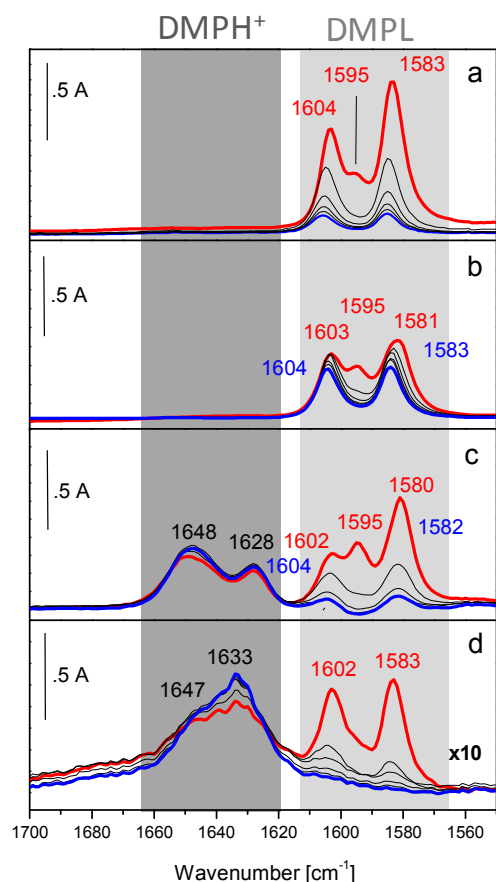


Fig.2. The IR spectral region of 8a-8b ring modes of 2,6-DMP. FTIR absorbance spectra after the interaction with 2 mbar of 2,6-DMP at r.t. (red curve) and during the outgassing (black and blue curves) with AuPtNPs on a) SiO<sub>2</sub>, b) MCM-41, c) S-ZrO<sub>2</sub>, d) H-Mordenite.

Adsorption microcalorimetry of NH<sub>3</sub> molecules was used to study the strength and the total amount of acid sites. Among the basic molecules, ammonia is a very convenient probe to determine the acid character, since it can interact with acidic hydroxyls forming ammonium ions. However, upon the neutralization of acidic hydroxyls next introduced ammonia molecules can react with ammonium ions (which also act as Brønsted acid sites), forming NH<sub>4</sub><sup>+</sup>×NH<sub>3</sub> dimers and as a consequence leading to an overestimation of the amount of Brønsted acid sites.<sup>9</sup> IR studies on dimers formation and decomposition within the pores of a TON zeolite demonstrated that the optimal temperature for ammonia adsorption is 400 K, because at this temperature only ammonium ions are formed.<sup>10</sup> Further FTIR experiments of NH<sub>3</sub> adsorption at 343 K on AuPt/H-Mordenite confirmed that no bands related to NH<sub>4</sub><sup>+</sup>×NH<sub>3</sub> dimers were observed (S8), therefore the microcalorimetric analyses have been performed at 373 K. In Figure 3 the calorimetric isotherm curves (section a) and the volumetric isotherm curves (section b) are reported.

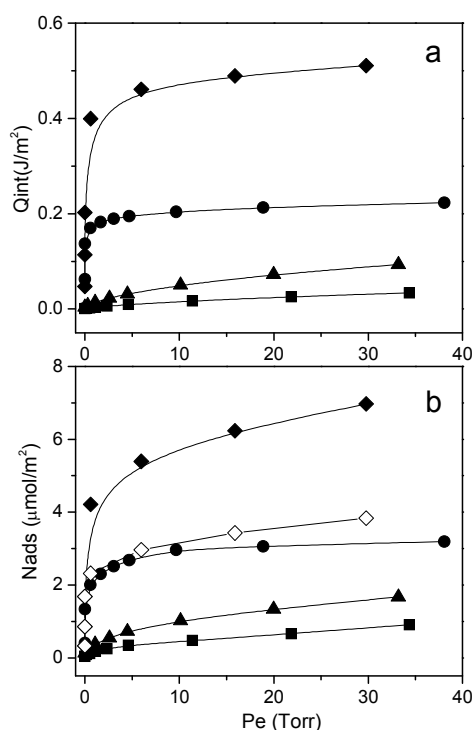


Fig.3 Section a: surface area-normalized calorimetric isotherms (integral heats vs. equilibrium pressure). Section b: surface area-normalized volumetric isotherms (mmol NH<sub>3</sub> adsorbed vs. equilibrium pressure). (-■-) AuPt/MCM-41; (-▲-) AuPt/SiO<sub>2</sub>; (-●-) AuPt/H-Mord; (-◆-) AuPt/S-ZrO<sub>2</sub>; (-◇-) AuPt/S-ZrO<sub>2</sub> without Lewis sites contribution.

The calorimetric isotherm provides the heat developed upon NH<sub>3</sub> adsorption,  $Q_{\text{int}}$  (J/m<sup>2</sup>) vs. the equilibrium pressure,  $P_e$  (Torr), allowing us to have information on the strength of the interaction between the molecule and the catalyst. In particular, as for equilibrium pressures ( $P_e$ ) up to 0.2 Torr, the developed heats follow the trend: AuPt/SiO<sub>2</sub> ≈ AuPt/MCM-41 < AuPt/S-ZrO<sub>2</sub> ≈ AuPt/H-Mordenite. This finding indicates that AuPt/S-ZrO<sub>2</sub> and AuPt/H-Mordenite expose acid sites that are stronger than those present on AuPt/SiO<sub>2</sub> and AuPt/MCM41, in agreement with the FTIR results, which revealed the presence of Brønsted acid sites on both catalysts supported on S-ZrO<sub>2</sub> and H-Mordenite and of silanol groups on the silica based systems.

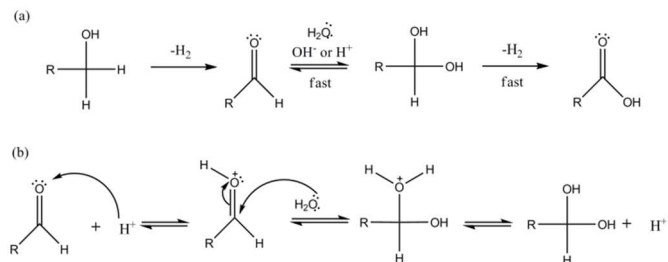
On the contrary, for  $P_e > 0.5$  Torr, the  $Q_{\text{int}}$  follows the sequence: AuPt/S-ZrO<sub>2</sub> > AuPt/H-Mordenite > AuPt/SiO<sub>2</sub> > AuPt/MCM-41. It has been frequently observed that the higher is the developed heat, the higher is the acidic strength of the site. In our case, the calorimetric isotherms (section a of Figure 3) display a quite similar trend if compared to that related to volumetric ones (reported in section b of Figure 3). Such feature allows us to state that the differences observed in the developed heats are directly correlated to the different amounts of adsorbed NH<sub>3</sub>. This is also confirmed by plotting the  $Q_{\text{int}}$  as function of the mmol of adsorbed NH<sub>3</sub> (S9).

Moreover, the volumetric isotherms can also provide information on the total amount of acid sites probed by ammonia, and the quantity of sites follows the order: AuPt/S-ZrO<sub>2</sub> > AuPt/H-Mordenite > AuPt/SiO<sub>2</sub> > AuPt/MCM41 (Table 1). However, we have to consider that the total amount of acid sites present on the surface of AuPt/S-ZrO<sub>2</sub> encompasses both Lewis and Brønsted sites. Therefore, in order to point out the role of different kinds of acid sites in the glycerol oxidation reaction, we have to discriminate between Lewis and Brønsted sites and to subtract the contribution due to Lewis sites from the total amount of acid sites. The relative abundance of Lewis/Brønsted sites can be determined by a quantitative analysis of the IR bands of adsorbed 2,6-DMP on AuPt/S-ZrO<sub>2</sub> (red curve in section c of Fig. 2). The deconvolution of the bands was carried out and the amount of acid sites was calculated by applying the Lambert-Beer Law (we used the following integrated molar absorption coefficients:  $\epsilon(\text{Brønsted}) = 6.5 \text{ cm mmol}^{-1}$ ,  $\epsilon(\text{Lewis}) = 3.4 \text{ cm mmol}^{-1}$ ).<sup>11</sup> It was found that the overall amount of sites exposed at S-ZrO<sub>2</sub> surface was composed of 55% - Brønsted sites and of 45% - Lewis sites. A new volumetric isotherm was built by subtracting the contribution of Lewis sites (Figure 3, section b, (-◇-)). This new curve reveals that on AuPt/S-ZrO<sub>2</sub> and AuPt/H-Mordenite catalysts the abundance of Brønsted sites is similar. The similar activity of the two catalysts, reported in Table 1, reported the importance of Brønsted and not of Lewis acid sites.

The characterization studies clearly show that the acidic surface properties of the catalysts affects both activity and selectivity. We also found that by increasing the number of acidic sites, a lower initial activity and more evident deactivation phenomena, occur. If we compare the trend in the catalytic activity, AuPt/H-Mordenite  $\approx$  AuPt/ZrO<sub>2</sub> < AuPt/SiO<sub>2</sub> < AuPt/MCM-41 (reported in Table 1), with the total amount of acid sites: AuPt/S-ZrO<sub>2</sub> > AuPt/H-Mordenite > AuPt/SiO<sub>2</sub> > AuPt/MCM-41 (data shown in Figure 3, section b) we find that the higher is the total amount of acid sites, the lower is the catalytic activity. AuPt/H-Mordenite and AuPt/S-ZrO<sub>2</sub> catalysts show similar activity, exposing a comparable abundance of Brønsted sites. In addition, AuPt supported on acidic oxides are the more efficient in term of selectivity to C3 products. Indeed, in all cases a selectivity to C3 >95% has been observed. Moreover, the C3 products distribution, in particular the amount of glyceraldehyde or glyceric acid detected, seems to be correlated not to their nature, but to the amount of acid sites and not to their nature. For AuPt/S-ZrO<sub>2</sub>, AuPt/H-Mordenite and AuPt/SiO<sub>2</sub> the main product is glyceric acid (53-61%) with a low amount of aldehyde (16-19%). On the contrary AuPt/MCM-41, which shows the lowest amount of acid sites, is able to stabilize glyceraldehyde, limiting its successive transformation to glyceric acid.

In order to prove it, AuPt/MCM41 and AuPt/H-Mordenite, as representative of the other acidic catalysts, were tested in the transformation of glyceraldehyde to glyceric acid, under the same reaction condition used for the glycerol oxidation (0.3 M glyceraldehyde, glyceraldehyde /metal = 500 mol/mol, 3 atm

O<sub>2</sub>, T = 80 °C). After 6 h of reaction AuPt/H-Mordenite completely converted the glyceraldehyde to glyceric acid whereas AuPt/MCM-41 showed a conversion of only 25%. These data are in agreement with the well accepted mechanism of aldehyde transformation to carboxylic acid via acid catalyzed diol formation and the subsequent rapid dehydrogenation to acid (scheme 2).<sup>3</sup>



Scheme 2 a) Alcohol dehydrogenation mechanism in presence of water and b) acid catalyzed geminal diol formation.

## Experimental

### Materials

NaAuCl<sub>4</sub>•2H<sub>2</sub>O, and K<sub>2</sub>PtCl<sub>4</sub> were from Aldrich (99.99% purity), H-Mordenite was from Degussa (SA = 450 m<sup>2</sup>/g), Sulphated zirconia (SA = 78 m<sup>2</sup>/g), SiO<sub>2</sub> (SA = 148 m<sup>2</sup>/g, P.V. 0.78 ml/g) and MgO (SA = 38 m<sup>2</sup>/g) were from Alfa Aesar. NiO (SA = 210 m<sup>2</sup>/g) and MCM-41 (SA = 980 m<sup>2</sup>/g) have been prepared following the procedure reported in ref. 12 and ref. 13, respectively. NaBH<sub>4</sub> of purity > 96% from Fluka, polyvinylalcohol (PVA) (M<sub>w</sub> = 13,000–23,000 87–89% hydrolyzed,) from Aldrich were used. A 1%wt PVA solution in water was prepared. Gaseous oxygen from SIAD was 99.99% pure.

### Catalyst preparation

MCM-41 mesoporous framework was prepared by a sol-gel method at RT by adopting the procedure described elsewhere (ref. 13). Typically, C<sub>16</sub>TAB (5.05 g, 0.014 mol) was dissolved in 100 ml of deionized water with a constant stirring (400 r.p.m). Subsequently, aq. ammonia solution (25% NH<sub>3</sub>, 37 ml, 0.5 mol) was added dropwise to the previous solution followed by the addition of 152 ml of absolute alcohol, as a co-solvent, and finally followed by the addition of 10 ml of TEOS, as a silica source. The solution turned turbid in one minute, then a bright white colloidal gel was formed. The solution was kept under constant stirring for 2 h, then aged at room temperature for 24 h. The resulting gel was filtered, washed with deionized water and dried at 363 K for 24 h. The template was removed by heating the dried gel to 823 K (1 K/min) in tube furnace for 8 h in flow of pure N<sub>2</sub>. For a complete removal of the template, the material was cooled down to RT, then flushed to pure O<sub>2</sub> and heated to 823 K (10 K/min) for 12 h.

NaAuCl<sub>4</sub>•2H<sub>2</sub>O (Au: 0.031 mmol) was dissolved in 60 mL of H<sub>2</sub>O, and PVA (1%, wt%) was added (Au/PVA = 1:0.5 wt/wt). The yellow solution was stirred for 3 min, after which 0.1 M NaBH<sub>4</sub> (Au/NaBH<sub>4</sub> = 1:4 mol/mol) was added under vigorous magnetic stirring. The ruby-red Au(0) sol was formed

immediately. Within a few minutes of sol generation, the gold sol was immobilized by adding the support (acidified to pH 2 by sulphuric acid) under vigorous stirring. The amount of support was calculated as having a gold loading of 0.60 wt%. After 2 h, the slurry was filtered and the catalyst washed thoroughly with distilled water (neutral mother liquors). The Au/support was dispersed in 40 mL of water, with  $K_2PtCl_4$  (Pt: 0.021 mmol) and PVA solution (Pt/PVA= 1:0.5 wt/wt) added.  $H_2$  was bubbled (50 mL/min) under atmospheric pressure and room temperature for 2 h. After an additional 18 h, the slurry was filtered and the catalyst washed thoroughly with distilled water. ICP analyses were performed on the filtrate using a Jobin Yvon JY24 instrument to verify the metal loading on the support. The total metal loading was 1 wt%.

### Oxidation of glycerol

Reactions were carried out in a thermostatted glass reactor (30 mL) provided with an electronically controlled magnetic stirrer connected to a large reservoir (5000 mL) containing oxygen at 3 atm. The oxygen uptake was followed by a mass flow controller connected to a PC through an A/D board, plotting a flow time diagram. The glycerol was dissolved in 10 mL of water, mixed the catalyst (0.3 M the final concentration of glycerol, glycerol/ metal = 500 mol/mol). The reactor was pressurized at 300 kPa of  $O_2$  and thermostatted at the appropriate temperature. Once the required temperature (40, 60, 80 °C) was reached, the gas supply was switched to oxygen and the monitoring of the reaction started. The reaction was initiated by stirring. Samples were removed periodically and analyzed by high-performance chromatography (HPLC) using a column (Alltech OA-10308, 300 mm x 7.8 mm) with UV and refractive index (RI) detection in order to analyze the mixture of the samples.  $H_3PO_4$  0.1% solution was used as the eluent. The identification of the possible products was done by comparison with the original samples. The presence of glyceraldehyde has been confirmed by NMR.  $^{13}C$  NMR spectra were recorded on a Bruker AC 300 NMR spectroscope. Water signal was suppressed using a low power PRESAT pulse in order to minimize signal distortions. 200  $\mu$ L of 0.3 M glyceraldehyde solution in  $H_2O$  were added to each sample (final volume 600  $\mu$ L). Products were recognised by comparison with authentic samples.

Recycling test: each run was carried out under the same conditions (0.3M glycerol, glycerol/metal=500 mol/mol, 3atm  $O_2$ , T=80°C, reaction time = 16h). The catalyst was recycled in the subsequent run after filtration without any further treatment.

### Catalyst characterization

The metal content was checked by ICP analysis of the filtrate on a Jobin Yvon JY24.

FTIR spectra were taken on a Perkin-Elmer 2000 spectrometer (equipped with a MCT detector) with the samples in self supporting pellets introduced in cells allowing thermal treatments in controlled atmospheres and spectrum scanning at room temperature (r.t.) in vacuum or in the presence of probe gases. From each spectrum, the spectrum of the sample before the inlet of the probe was subtracted. The standard IR experiment of 2,6-DMP adsorption/ desorption on the various samples, previously activated in vacuum at 393 K, was carried out as follows: (i) allowance in the IR cell of an excess dose of 2,6-DMP vapor ( $\approx 2$  Torr), and equilibration at room temperature for 10 min; (ii) evacuation of the IR cell at r.t. for 15 min.

Microcalorimetric measurements were run on a Tian-Calvet heat flow calorimetric equipment (Setaram C80d). Each sample was pretreated in vacuum (10<sup>-5</sup> Torr) at 393 K (as for IR experiments) and then contacted with successive small doses of  $NH_3$  vapour at 373 K. The first adsorption runs (primary isotherms) were stopped at a final equilibrium pressure of 35 Torr. The primary adsorption isotherms were followed by a prolonged outgassing at the adsorption temperature and then by a second adsorption run up to the same final  $NH_3$  pressure (secondary isotherms). Uptake differences between primary and secondary isotherms are usually considered to monitor the occurrence and the extent of irreversible adsorption processes. Samples were prepared for TEM characterisation by dispersing the catalyst powder in high purity ethanol, followed by sonication. A drop of this suspension was then evaporated on a holey carbon film supported by a 300 mesh copper TEM grid. Samples were then subjected to bright field diffraction contrast imaging experiments in order to image the particles. The instrument use for this analysis was a JOEL-2100 LaB6 TEM operating at 200kV. High resolution transmission microscopy (HRTEM) analysis was performed using a side entry Jeol JEM 3010 (300 kV) microscope equipped with a LaB6 filament and fitted with X-ray EDS analysis by a Link ISIS 200 detector. All digital micrographs were acquired by an Ultrascan 1000 camera and the images were processed by Gatan digital micrograph. X Ray Powder Diffraction data were obtained by using a Rigaku DMAX Diffractometer with Cu KR radiation operating at 40 keV and 40 mA, with a 0.05° divergence slit; spectra were recorded in the range 1-8°.

### Conclusions

Supported AuPt nanoparticle catalysts were tested in the base-free glycerol aqueous phase oxidation, using supports with different acid-base properties. The catalytic behavior is markedly influenced by the support with respect to both activity and selectivity. Basic supports (MgO, NiO) promote the activity but also increase the C-C bond cleavage reactions thus decreasing the selectivity to the desired products. On the contrary, acidic supports showed a higher selectivity to  $C_3$  oxidation products. Spectroscopic and microcalorimetric measurements provided evidence that the catalytic activity and selectivity are not influenced by the nature of acid sites, but to their amount. In particular, both activity and selectivity to glyceraldehyde decrease by increasing the number of acid sites (Brønsted sites and/or silanols). Indeed, the successive transformation of glyceraldehyde to glyceric acid proceeds via an acid catalyzed geminal diol formation and its dehydrogenation carboxylic acid. Moreover, Lewis acid sites seem not to be involved.

### Acknowledgements

We are grateful to the Research Complex at Harwell for the provision of several of the facilities used in this work and to the EPSRC for studentship funding to WJ.

### Notes and references

<sup>a</sup> Università di Milano, Dipartimento di Chimica, via Golgi 19, I-20133Milano, Italy.

E-mail:Laura.prati@unimi.it

<sup>b</sup> School of Chemistry, Southampton University, SO171BJ, UK.

<sup>c</sup> University College London, 20 Gordon Street, WC1H 0AJ London, UK.

<sup>d</sup> Dipartimento di Chimica and NIS Centre of Excellence, Università di Torino, Via P.Giuria 7, 10125 Torino, Italy.

<sup>e</sup> School of Chemistry, Cardiff University, Main Building, Park Place, Cardiff, CF103AT

<sup>f</sup> UK Catalysis Hub, Research Complex at Harwell (RCaH), Rutherford Appleton

Laboratory, Harwell, Oxon, OX11 0FA, UK

<sup>g</sup> Chemistry Department, Faculty of Science, Sohag University, P. O. Box 82524, Sohag, Egypt.

Electronic Supplementary Information (ESI) available: [Reaction profiles and temperature effect in glycerol oxidation, NMR characterization, and additional data for calorimetric tests.]. See DOI: 10.1039/b000000x/

- 1 a) G. W. Huber, S. Iborra, A. Corma, *Chem. Rev.*, 2006, **106**, 4044; b) A. Corma, S. Iborra, and A. Velty, *Chem. Rev.*, 2007, **107**, 2411; c) P. Gallezot, *Chem. Soc. Rev.*, 2012, **41**, 1538
- 2 a) C.-H. Zhou, J. N. Beltramini, Y.-X. Fan, G. Q. Lu, *Chem. Soc. Rev.*, 2008, **37**, 527; b) B. Katryniok, H. Kimura, E. Skrzyńska, J.-S. Girardon, P. Fongarland, M. Capron, R. Ducoulombier, N. Mimura, S. Paul, F. Dumeignil, *Green Chem.*, 2011, **13**, 1960; c) M. Simoes, S. Baranton, C. Coutanceau, *Chem. Sus. Chem.*, 2012, **5**, 2106; d) S. E. Davis, M. S. Ide, R. J. Davis, *Green Chem.*, 2013, **15**, 17.
- 3 a) M. Bessom, P. Gallezot, *Catal Today*, 2000, **57**, 127; b) T. Mallat and A. Baiker, *Chem. Rev.*, 2004, **104**, 3037; c) N. Dimitratos, J. A. Lopez-Sanchez, G. J. Hutchings, *Chem. Sci.*, 2012, **3**, 20.
- 4 a) S. Carrettin, P. McMorn, P. Johnston, K. Griffin, C. J. Kiely, G. J. Hutchings, *Phys. Chem. Chem. Phys.*, 2003, **5**, 1329; b) F. Porta and L. Prati, *J. Catal.*, 2004, **224**, 397; c) S. Demirel-Gulen, M. Lucas, P. Claus, *Catal. Today*, 2005, **102-103**, 166.
- 5 a) A. Villa, G. M. Veith and L. Prati, *Angew. Chem. Int. Ed.*, 2010, **49**, 4499; b) G. L. Brett, Q. He, C. Hammond, P. J. Miedziak, N. Dimitratos, M. Sankar, A. A. Herzing, M. Conte, J. A. Lopez-Sanchez, C. J. Kiely, D. W. Knight, S. H. Taylor, and G. J. Hutchings, *Angew. Chem. Int. Ed.*, 2010, **50**, 10136; c) D. Liang, J. Gao, H. Sun, P. Chen, Z. Hou, X. Zheng, *Appl. Catal. B: Environmental*, 2011, **106**, 423; d) R. Niea, D. Lianga, L. Shenb, J. Gaoa, P. Chena, Z. Hou, *Appl. Catal. B: Environmental*, 2012, **127**, 212; e) D. Tongsakul, S. Nishimura, and K. Ebitani, *ACS Catal.*, 2013, **3**, 2199; f) S. A. Kondrat, P. J. Miedziak, M. Douthwaite, G. L. Brett, T. E. Davies, D. J. Morgan, J. K. Edwards, D. W. Knight, C. J. Kiely, S. H. Taylor and G. J. Hutchings, *ChemSusChem*, 2014, **7**, 1326.
- 6 C. Morterra, G. Meligrana, G. Cerrato, V. Solinas, E. Rombi, M. F. Sini, *Langmuir*, 2003, **19**, 5344.
- 7 C. Morterra, G. Cerrato, G. Meligrana, *Langmuir*, 2001, **17**, 7053.
- 8 D. Stošić, S. Bennici, J.-L. Couturier, J.-L. Dubois, A. Auroux *Catal. Comm.*, 2012, **17**, 23.
- 9 A. Zecchina, L. Marchese, S. Bordiga, C. Paze, E. Gianotti, *J. Phys. Chem.* 1997, **101**, 1012.
- 10 J. Datka, K. Go'ra-Marek *Catalysis Today*, 2006, **114**, 205-210
- 11 T. Onfroy, G. Clet, M. Houalla, *Microp. Mesop. Mat.*, 2005, **82**, 99.
- 12 A. Villa, C. E. Chan-Thaw, G. M. Veith, K. L. More, D. Ferri, L. Prati, *Chem. Cat. Chem.*, 2011, **3**, 1612.
- 13 K. M. S. Khalil, *J. Colloid Interf. Sci.*, 2007, **315**, 562-568.